e^+/e^- discrimination in liquid scintillator and its usage to suppress ^{8}He/^{9}Li backgrounds *

Ya-Ping Cheng(程雅苹)[1,2;1)] Liang-Jian Wen(温良剑)[2;2)] Peng Zhang(张鹏)[2] Xing-Zhong Cao(曹兴忠)[2]

[1] University of Chinese Academy of Sciences, Beijing 100049, China
[2] Institute of High Energy Physics, Chinese Academy of Sciences, Beijing 100049, China

Abstract: Reactor neutrino experiments build large-scale detector systems to detect neutrinos. In liquid scintillator, a neutral bound state of a positron and an electron, named positronium, can be formed. The spin triplet state is called ortho-positronium (o-Ps). In this article, an experiment is designed to measure the lifetime of o-Ps, giving a result of 3.1 ns. A PSD parameter based on photon emission time distribution (PETD) was constructed to discriminate e^+/e^-. Finally, the application of e^+/e^- discrimination in the JUNO experiment is shown. It helps suppress ^{8}He/^{9}Li backgrounds and improves the sensitivity by 0.6 in χ^2 analysis with an assumption of σ=1 ns PMT Transit Time Spread, which will bring a smearing effect to the PETD.

Keywords: PSD, LS, ortho-positronium

PACS: 36.10.Dr, 29.40.Mc, 78.70.Bj **DOI:** 10.1088/1674-1137/41/1/016101

1 Introduction

In most reactor neutrino experiments, electron antineutrinos are detected via the inverse β-decay (IBD) reaction, $\bar{\nu}_e + \mathrm{p} \rightarrow \mathrm{e}^+ + \mathrm{n}$. The antineutrino signature is a coincidence between the prompt positron signal and the microseconds-delayed neutron capture on the target (proton or doped isotope). The most serious background is the cosmogenic ^{8}He/^{9}Li background, which can mimic the IBD signature via a β+n cascade decay. Thus, the capability of positron-electron discrimination is extremely useful to reject the ^{8}He/^{9}Li background.

Prior to annihilation, the positron can form a neutral bound state of a positron and an electron, namely positronium. The formation threshold of positronium is 6.75 eV [1]. Depending on the total spin angular momentum, positronium is classified into the spin singlet para-positronium (p-Ps) state and the spin triplet ortho-positronium (o-Ps) state. In vacuum, the p-Ps state annihilates by emitting two γ rays of 511 keV with a mean lifetime of 125 ps, while the o-Ps state emits three γ rays with a mean lifetime of ∼140 ns. In liquid scintillator (LS), the mean lifetime of o-Ps state is strongly reduced to a few nanoseconds due to the interactions of o-Ps with the surrounding medium [2]. The o-Ps in different LS solvents has slightly different lifetimes and formation probabilities [3].

The delay of positron annihilation can induce distortion in the photon emission time distribution (PETD) of the detected photons. In addition, the two annihilation gamma rays will further induce distortion to the PETD due to Compton scattering. The PETD difference between positrons and electrons provides an opportunity for positron-electron discrimination in LS detector and the consequent rejection of ^{8}He/^{9}Li background from IBD candidates.

In this paper, we study the potential mass hierarchy sensitivity improvement of the Jiangmen Underground Neutrino Observatory (JUNO) ([4, 5]) by positron-electron discrimination analysis. JUNO is a 20 kton multi-purpose liquid scintillator detector, with the primary goal to determine the neutrino mass hierarchy by detecting reactor antineutrinos. The JUNO central detector uses linear alkyl-benzene (LAB)-based LS and has excellent energy resolution of $\sim 3\%/\sqrt{E}$. The energy scale is about 1200 photoelectron/MeV and the PMT photocathode coverage is about 78%. The outline of this article is as follows. In Section 2 a newly designed apparatus for positron annihilation lifetime measurement is presented. In Section 3 the measured o-Ps lifetime in LAB is reported. Section 4 describes a pulse shape discrimination (PSD) method for positron-electron discrimination. Finally, the application of positron-electron discrimination to JUNO and the improvement on mass

Received 15 Apr 2016, Revised 27 July 2016

∗ Supported by National Natural Science Foundation of China (11575226, 11475197, 11205183)

1) E-mail: chengyp@mail.ihep.ac.cn

2) E-mail: wenlj@mail.ihep.ac.cn

hierarchy sensitivity is shown in Section 5.

2 Positron lifetime measurement experimental apparatus

A Positron Annihilation Lifetime Spectroscopy (PALS) apparatus, developed in-house, was used to measure the o-Ps formation fraction and its lifetime. A schematic diagram of the experimental setup, and the electronics and data acquisition (DAQ) scheme, are shown in Fig. 1. The notations in Fig. 1(b) are as follows: CFDD: constant fraction differential discriminator; SCA: single channel analyzer; TAC: time-to-amplitude converter; MCA: multichannel amplitude analyzer.

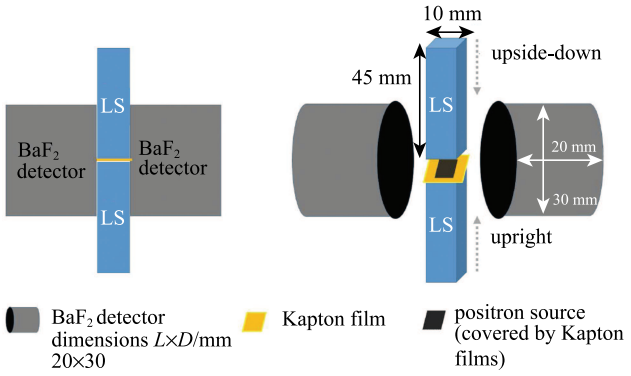

(a) Schematic diagram of the experimental setup
(Left: side view of the setup
Right: dimensions of each constituent part)

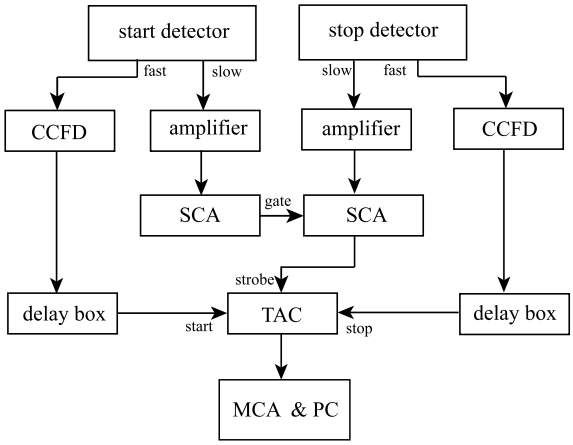

(b) Electronics and data acquisition scheme

Fig. 1. Experimental apparatus

Typically the sample for the PALS is crystal or powder pressed into thin slices. To measure the positron annihilation in the LAB liquid, a special design was developed. A thin positron source was made of a dried drop of liquid NaCl encapsulated in two layers of 7.5 μm Kapton films, with ^{22}Na serving as the positron source. Over 90% of radioactive ^{22}Na decays by emission of a positron to the excited state of ^{22}Ne, then immediately reaches the ground state by emission of a 1.274 MeV γ. The kinetic energy spectrum of positron is a continuous distribution ranging from 0 to 545 keV and the activity of the positron source was 15 μCi. The LS sample was placed in a disposable Brand cuvette [6] made of acrylic material which is completely compatible with LS. Each cuvette had a capacity of 4.5 mL (10 mm × 10 mm × 45 mm) with no lid, and was 1 mm thick, sealed by a piece of thin Kapton film. The two cuvettes were stacked vertically with the flat positron source placed in between the two films. The top cuvette was placed upside-down, and the bottom cuvette placed upright. Two BaF_2 plastic scintillators (dimensions $L \times D$: 20 mm × 30 mm) coupled with 2-inch PMTs (type: XP2020Q) were covered by black film, placed at opposite sides of the cuvettes, and used to measure the 511 keV annihilation γ and the 1.27 MeV γ. The DAQ system was a fast-slow coincidence system. The BaF_2 crystal emits both fast and slow scintillation components. The decay time of fast and slow components is ∼600 ps and ∼630 ns respectively, and their intensities are ∼15% and ∼85% respectively. The fast coincidence channel was for time measurement. The fast component signals from the BaF_2 detectors, which served as the timing signal, were passed to the input of a constant fraction differential discriminator (CFDD). The slow signals from the BaF_2 detectors were fed to the slow coincidence channel. Two single channel analyzers (SCAs) were used to select γs over the energy range of 1.27 MeV and 511 keV. The 1.27 MeV γ from ^{22}Na decay served as the start signal, and the 511 keV γ from positron annihilation served as the stop signal. The appropriate γs generated the strobe signal for the time-to-amplitude converter (TAC). The analog pulse proportional to the time interval between the start and stop pulses was fed to the multichannel amplitude analyzer (MCA) and converted into a digital signal, then stored on data disk for later analysis.

3 Data taking and data analysis

Oxygen dissolved in liquid scintillator can decrease the positron annihilation lifetime. To remove oxygen in the test sample, we bubbled the sample with high purity nitrogen for about 40 minutes. The flow rate of nitrogen was carefully controlled by a pressure reducing valve. The time interval between the 511 keV γ from positron annihilation and the 1.27 MeV γ which accompanies the sodium β^+ decay was taken as the lifetime of the positron. The time resolution of the system was 190 ps (FWHM) calibrated by the two instantaneous γ rays of a cobalt-60 source.

The o-Ps lifetime was extracted from the measured lifetime spectrum using the RooFit [7] tool. The positron

annihilation lifetime in LS can be described as the sum of two exponential components. The short-lived p-Ps and directly annihilating positron are indistinguishable, therefore they are merged into one component, denoted as τ_0 in Eq. (1). The other component represents o-Ps, shown as τ_1 in Eq. (1). The formation probability of o-Ps is represented by w in Eq. (1). Positron annihilation in the substrate material also contributes to the measured lifetime spectrum. This can be described by two exponential components. One originates from the Kapton, denoted as τ_{0s}. The other component is generated from contaminants in the positron source, denoted as τ_{1s}. Similarly, the relative weight of these two components is shown as w_s. The percentage of positron annihilation in the source is evaluated by I_s in Eq. (1). The system instrumental time resolution is assumed as a Gaussian distribution. Using σ and T to represent the instrumental time resolution and time latency, and t' as the convolution operation sign, the final fitting function is shown as Eq. (1).

$$F(t)=\int_0^t \frac{N}{\sqrt{2\pi}\sigma}\mathrm{e}^{-\frac{t-T-t'}{2\sigma^2}}\left\{(1-I_s)\times\left(\frac{1-\omega}{\tau_0}\mathrm{e}^{-\frac{t'}{\tau_0}}+\frac{\omega}{\tau_1}\mathrm{e}^{-\frac{t'}{\tau_1}}\right)+I_s\times\left(\frac{1-\omega_s}{\tau_{0s}}\mathrm{e}^{-\frac{t'}{\tau_{0s}}}+\frac{\omega_s}{\tau_{1s}}\mathrm{e}^{-\frac{t'}{\tau_{1s}}}\right)\right\}\mathrm{d}t'. \quad (1)$$

The Life Time 9.0 program [8] (LT9), based on the least squares fitting method, was used as a crosscheck. Their difference was taken as the error in the measured positron annihilation lifetime. In this measurement, optical photons were shielded by the black film and only γs can propagate into the BaF_2 detector, thus in the measured lifetime spectrum there is no contribution from the LS sample's scintillation light.

A standard sample made from nickel was measured first, and the effects of the source substrate were obtained by fitting the measured lifetime spectrum of nickel. The positron annihilation lifetime in nickel is described by one exponential component and known to be about 108 ps [9]. The results from LT9 and RooFit were 117 ps and 112 ps respectively. The source effects are generated from Kapton and other impurities. Positron annihilation lifetime in impurities (τ_{1s}) and w_s were fixed by the value from nickel fitting. τ_{0s}, the positron lifetime in Kapton, was treated as a floating parameter. In the fitting for the nickel sample, τ_{0s} was 385 ps. In the fitting for the LAB sample, τ_{0s} was about 382 ps. The positron lifetime in impurities τ_{1s} and its intensity w_s were 1.095 ns and 11.88% respectively. I_s, the percentage of positrons lost in the positron source (Kapton or other impurities), was about 50.34%. τ_0, the lifetime of p-Ps or directly annihilating positrons, was 150 ps. The positron annihilation lifetime spectrum in LAB is shown in Fig. 2. The top panel shows the measured and fitted lifetime spectrum. The bottom panel shows the residual between data and fit normalized to the statistical Poisson error of fit counts. From the unfolding result, the o-Ps lifetime is about 3.10 ± 0.07 ns and its formation probability is about $(43.7\pm1.2)\%$.

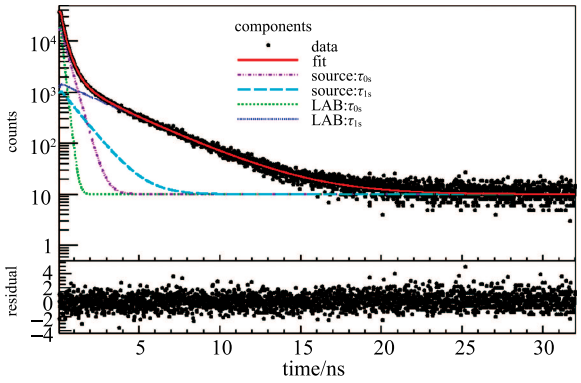

Fig. 2. The measured and fitted lifetime spectra of positron annihilation in LAB.

4 Simulation and PSD performance

Based on the measurement result described in the previous section, we studied the e^+/e^- discrimination power by simulation. The simulation was done using the JUNO simulation framework SNiPER [10], in which the positronium production process is not included in the physics list. Therefore, for simplicity, a tag on photons generated directly from the positron annihilation process was created. We did a sampling based on o-Ps formation probability 43.7% and lifetime 3.1 ns. The sampling result served as the delay to photon emission time caused by o-Ps for those tagged photons. Under such assumptions, taking positrons and electrons with deposited energy 2.5 MeV as an example, we got the averaged time profile for positron and electron as Fig. 3. The time profile was determined by measuring the arrival times of both early and late hits on each PMT in one event.

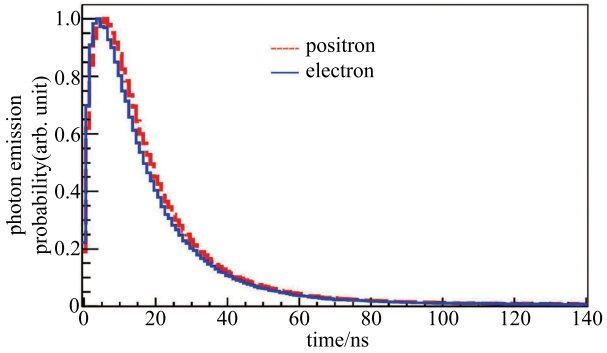

Fig. 3. Photon emission time profile for 2.5 MeV positrons and electrons as an example

To exploit the difference, we created PSD parameters. Two PSD parameters were constructed to do e^+

and e^- discrimination. One parameter is the tail to total ratio in the PETD. The start of the tail was chosen to be 10 ns and the total time window was chosen to be 50 ns. The other parameter is the optimum Gatti parameter [11] defined as Eq. (2). Here $r_i(t_n)$ denotes the photon emission probability in the time interval t_{n-1} to t_n for the unknown particle. The weight $w(t_n)$ was calculated using e^+ photon emission probability ($r_1(t_n)$) and e^- photon emission probability ($r_2(t_n)$). The performance of the tail to total ratio parameter was not as good as the Gatti parameter, so it was not used.

$$G=\sum_n r_i(t_n)w(t_n), \tag{2}$$

$$r_i(t_n)=\int_{t_{n-1}}^{t_n} P_i(t)\mathrm{d}x \qquad w(t_n)=\frac{r_1(t_n)-r_2(t_n)}{r_1(t_n)+r_2(t_n)}.$$

Besides these two PSD parameters, an artificial neutral network method was also investigated. The multilayer perceptron (MLP) algorithm from the ROOT Toolkit for Multivariate Data Analysis [12] was used. Such an algorithm yields an output qualifier indicating the particle type. The input to the algorithm comprises 16 variables, defined as follow. We build the cumulative distribution function of the PETDs, and we set 16 thresholds equally distributed between 0.03 and 0.33. The time values at which the threshold crossings occur serve as input variables. The total number and the values of the thresholds were optimised to sample the PETD range with the most discrimination power. The training and test samples are every other two entries in the ROOT tree file.

A figure of merit (FOM) parameter was used to evaluate the PSD parameter discrepancy of positron and electron. FOM was defined as the peak distance divided by the summation of FWHM of each particle. We applied the Gatti parameter and MLP algorithm on positron and electron Monte Carlo samples, and found that the Gatti parameter and MLP had similar performance. An example is shown in Fig. 4. The electron and positron energy was 4.5 MeV, the Gatti FOM was 0.265 and the MLP FOM was 0.266. The following analysis is based on the Gatti discrimination parameter.

In consideration of the following studies, e^+/e^- discrimination power at different energies was studied. The energy range extended from 1.0 MeV (the minimum deposited energy of the positron) to 9.0 MeV. In this study $\sigma=1$ ns PMT Transit Time Spread (TTS) was added to the PETD of positron and electron. The smearing effect on PETD from vertex resolution was much less severe. A 10 cm vertex reconstruction resolution was applied. The e^+/e^- discrimination at different energies is shown in Fig. 5.

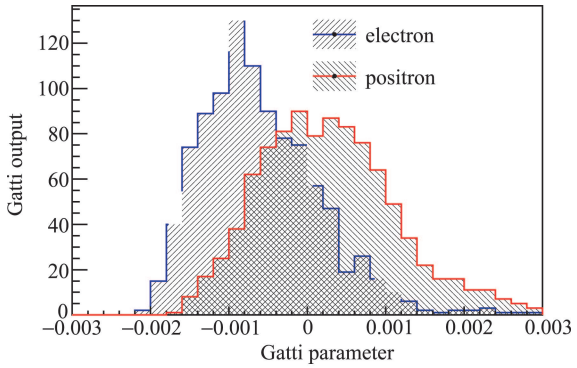

(a) PSD output by Gatti parameter

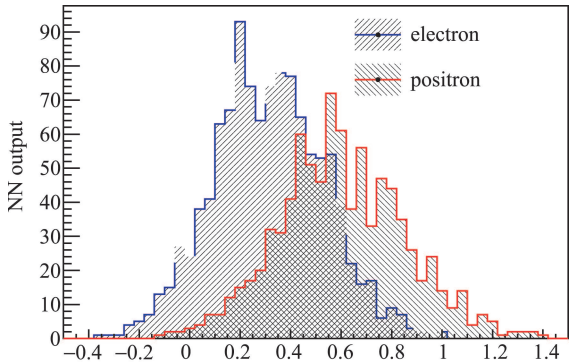

(b) PSD output by MLP neural network

Fig. 4. PSD performance of Gatti parameter and MLP

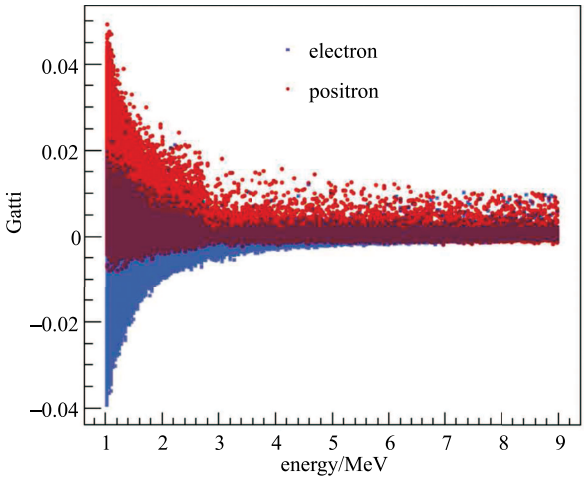

Fig. 5. Gatti parameter distribution for e^+ and e^- at different energies

5 PSD application in the JUNO experiment

^{8}He and ^{9}Li can mimic IBD interactions. The prompt signal includes the contributions from electron, α, and the recoil energy of the neutron. The delayed signal is the neutron capture signal. Since the electron contributes ~90% of the prompt signal's visible energy and

the PETD changes less than 0.5% compared with pure electron signals, in this study, the electron was taken as the prompt signal. Since the ^{8}He and ^{9}Li isotopes are mainly produced by cosmic muons going through the detector, a veto on the detector volume within a time window since the last muon can be applied to reject the ^{8}He/^{9}Li background. This veto strategy was studied in [5]. For example, a veto cut to reject the detector volume within a cylinder with distance from muon track less than 3 meters in a 1.2 s time window since the last muon can reduce this background from 71/day to 1.6/day. However, the IBD event rate is also reduced by 17% due to the dead time caused by the veto. The PSD in this study can be used as another method to reject ^{8}He/^{9}Li background. With the help of the PSD method, the veto cut can be loosened to reduce the dead time without sacrificing signal to background ratio. To evaluate the improvement of the mass hierarchy sensitivity by optimizing the PSD and veto conditions, a χ^2 was defined as Eq. (3), where i is the bin index of the spectra, M^i is the simulated spectrum including IBD signal (S^i) and background (B_b^i), and F^i is the fit spectrum with the oscillation parameters to be fitted. $\varepsilon_R, \varepsilon_r, \varepsilon_B$ are nuisance parameters corresponding to the reactor flux and detector efficiency normalization factor, reactor uncorrelated uncertainty (σ_r), and background rate uncertainty (σ_B). The spectrum shape uncertainties due to the IBD signal and background are included by introducing σ_{b2b} and σ_b.

$$\chi^2 = \sum_i^{N_{\rm bin}} \frac{(M^i - F^i)^2}{M^i + (\sigma_{b2b} S^i)^2 + \sum_{Bkg}(\sigma_b B_b^i)^2} + \sum_{Bkg}\left(\frac{\varepsilon_B}{\sigma_B}\right)^2 + \sum_r \left(\frac{\varepsilon_r}{\sigma_r}\right)^2 \quad (3)$$

$$F^i = S^i\left(1+\varepsilon_R+\sum_r w_r\varepsilon_r\right)+\sum_{Bkg} B_b^i(1+\varepsilon_B)$$

The simulated spectrum M^i is calculated assuming either normal hierarchy (NH) or inverted hierarchy (IH) without statistical fluctuations. When the fit spectrum uses the same assumption, the minimization of the χ^2 over the oscillation parameters and nuisance parameters yields 0. While assuming the opposite mass hierarchy in the fit spectrum, we obtain $\chi^2_{\rm min}$. The sensitivity of the mass hierarchy can be expressed as $\Delta\chi^2 = \chi^2_{\rm min} - 0$.

The neutrino spectra after applying PSD analysis served as the input for the χ^2 analysis. The PSD cut efficiency at each energy bin of the IBD prompt and background spectrum was calculated by using mono-energetic MC e^-/e^+ samples. Since we use the neutrino spectrum in the χ^2 analysis, we need to do a transformation between the prompt energy and neutrino energy to get the corresponding efficiency at the neutrino spectrum bin. The conversion was done according to equation 11 in [13]. The PSD efficiencies were applied on M^i, S^i and the specific B_b^i corresponding to ^{8}He/^{9}Li in Eq. (3). The PSD cut efficiency errors were taken as uncorrelated systematic errors and were added in quadrature to σ_{b2b} and σ_b in Eq. (3).

In the $\Delta\chi^2$ calculation, we scanned the PSD cut and veto conditions. The tested veto schema included a combination of volume veto cylinder radius 1.6 m, 2 m, 3 m and veto time 0.7 s, 1 s, and 1.3 s. One optimized muon veto scheme that gave good χ^2 was to veto the detector volume within a cylinder with distance from the muon track less than 2 m in a 1.0 s time window. We can improve the χ^2 from the original 10.60 without PSD analysis to 11.17 after PSD analysis. The signal and background Gatti parameter distributions are shown in Fig. 6.

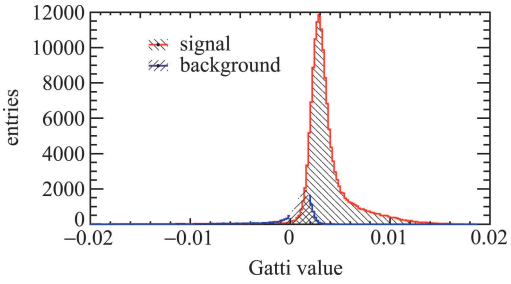

Fig. 6. Mixed Gatti parameter distribution

Figure 7 shows the signal and background efficiency under the optimized Gatti parameter cut (−0.001). In each energy bin, 4000 events were used and the statistical uncertainty was calculated by carrying out the Bayesian approach, treating the number of passing events as a binomially distributed variable, with uniform prior probability assumption for the cut efficiency, shown as the error bars in Fig. 7. The errors in Fig. 7 are enlarged 10 times to be seen clearly. In future, the PSD efficiency and uncertainties can be derived from a data-driven analysis.

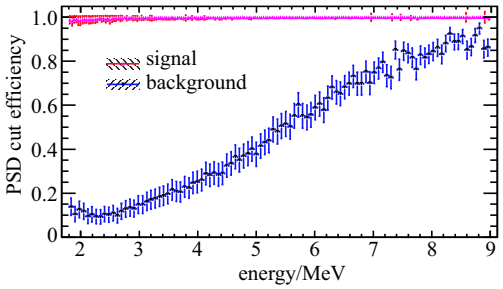

Fig. 7. Signal and background efficiency under the optimized Gatti parameter cut, with efficiency error enlarged 10 times

6 Conclusion

We have measured the lifetime and formation probability of ortho-positronium. In oxygen-free LAB, the

o-Ps lifetime is 3.10 ± 0.07 ns and its formation probability is (43.7 ± 1.2)%. The backgrounds in this design scheme were calibrated by testing standard samples.

We performed simulations under the framework SNiPER. We assumed the PMT TTS was 1 ns and the energy scale was about 1200 photoelectron/MeV, and we applied e^+/e^- PSD to reduce ^{8}He/^{9}Li backgrounds. From the MH sensitivity study, by loosening the muon veto cut and instead using PSD analysis to reject the ^{8}He/^{9}Li backgrounds, χ^2 improvements can be made. For example, vetoing the detector volume within 2 meters in a 1.0 s time window can improve the final χ^2 from 10.60 (w/o PSD) to 11.06 (w/PSD).

The authors would like to thank Dr. Liang Zhan for the helpful χ^2 discussions, Dr. Miao He for his useful comments and Dr. Marco Grassi for his kindly language editing help.

Appendix A

Positron annihilation lifetime in nickel

Positron annihilation lifetime in nickel was described by one exponential component τ_{ni}, instead of both τ_0 and τ_1 as shown in Eq. (1). The measured and fitted spectra are shown in Fig. A1. The top panel shows the measured and fitted lifetime spectrum, with the bottom panel showing the residual.

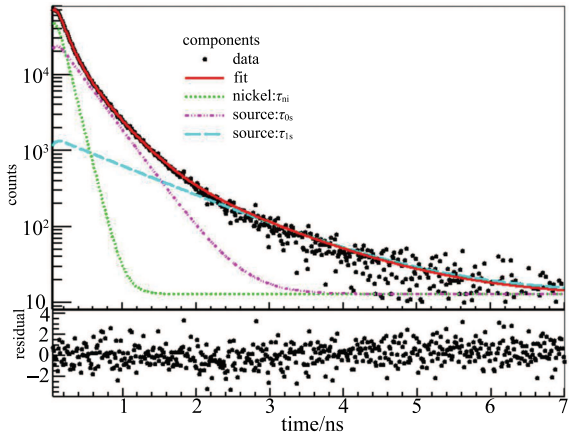

Fig. A1 The measured and fitted lifetime spectra of positron annihilation in nickel

References

1 B. H. Bransden and Z. Jundi, PROC. PHYS. SOC, **92**: 880 (1967)
2 D. Franco, G. Consolati, and D. Trezzi, Phys. Rev. C, **83**: 015504 (2011)
3 G. Consolati et al, Phys. Rev. C, **88**: 065502 (2013)
4 Z. Djurcic et al (JUNO Collaboration), arXiv: 1508. 07166
5 F. P. An et al (JUNO Collaboration), J. Phys. G, **43**: 030401 (2016)
6 http://www.brandtech.com/prodpage.asp?prodid=759070D, retrieved 29th April 2016
7 W. Verkerke et al, arXiv: physics/0306116v1
8 J. Kansy, Nucl. Instrum. Methods A, **374**: 235 (1996)
9 Wenshuai Zhang et al, Computational Materials Science, **105**: 32 (2015)
10 J. H. Zou et al, J. Phys. Conf. Ser., **664**(7): 072053 (2015)
11 E. Gatti and F. De Martini, Nuclear Electronics IAEA. Vienna, **2**: 265–276 (1962)
12 Hoecker A et al, arXiv: physics/0703039
13 P. Vogel and J. F. Beacom, Phys. Rev. D, **60**: 053003 (1999)